Theoretical Study of the Thermolysis Reaction of Ethyl β-Hydroxycarboxylates in the Gas Phase

ARTICLE *in* THE JOURNAL OF PHYSICAL CHEMISTRY A · MAY 2002

Impact Factor: 2.69 · DOI: 10.1021/jp020071f

7 AUTHORS, INCLUDING:

Eduardo Chamorro
Universidad Andrés Bello
79 PUBLICATIONS **1,690** CITATIONS

SEE PROFILE

Theoretical Study of the Thermolysis Reaction of Ethyl β-Hydroxycarboxylates in the Gas Phase

Rafael Notario,*,† Jairo Quijano,‡ J. Camilo Quijano,‡ Luisa P. Gutiérrez,‡ Wilmar A. Suárez,‡ Claudia Sánchez,‡ Luis A. León,‡ and Eduardo Chamorro§

Instituto de Química Física "Rocasolano", C.S.I.C., Serrano 119, 28006 Madrid, Spain, Laboratorio de Fisicoquímica Orgánica, Escuela de Química, Universidad Nacional de Colombia, Sede Medellín, Apartado Aéreo 3840, Medellín, Colombia, and Departamento de Física, Facultad de Ciencias, Universidad de Chile, Santiago, Chile

Received: January 11, 2002; In Final Form: March 1, 2002

Theoretical studies on the thermolysis of three ethyl β-hydroxycarboxylates in the gas phase were carried out using ab initio theoretical methods, at the MP2/6-31G(d) and MP2/6-311++G(2d,p)//MP2/6-31G(d) levels of theory. Two competitive reaction pathways for the decomposition process have been studied. The first pathway describes a two-step mechanism, with the formation in a first step of an aldehyde, or a ketone, and an enol intermediate, followed by the tautomerization of this intermediate to ethyl acetate. The second pathway is a one-step mechanism with formation of ethylene and a carboxylic acid. Both processes occur via six-membered cyclic transition states. The thermolysis is favorable along the first pathway with the first step as the rate-limiting step for the global process. The progress of the principal reactions was followed by means of the Wiberg bond indices. The results indicate that the transition states are late, and the calculated synchronicities show that the reactions are concerted and highly synchronous. The bond-breaking processes are more advanced than the bond-forming ones indicating a bond deficiency in the transition states. The kinetic parameters calculated for the studied reactions agree very well with the available experimental results. A theoretical study on the kinetic deuterium isotope primary, and α- and β-secondary, effects has also been carried out.

Introduction

Ethyl β-hydroxycarboxylates, $R_1R_2C(OH)CH_2COOEt$, decompose thermally in the gas phase and in *p*-xylene solution to a mixture of aldehydes and/or ketones and ethyl acetate.[1−4] Small amounts of ethylene and carboxylic acid (<5%) were detected in a temperature range of 296−330 °C and a pressure range of 29−108 Torr.[4]

The suggested mechanism of their decomposition process is shown in Figure 1, where R_1 and R_2 represent $-CH_3$ and/or −H.

It was proposed that the reaction involves a cyclic six-membered transition state similar to that thought to be involved in other thermal decompositions such as the thermolysis of β-hydroxyketones[5,6] ($R_1R_2C(OH)CH_2COCH_3$), β-hydroxyolefins[7] ($R_1R_2C(OH)CH_2CH{=}CH_2$), and β-hydroxyacetylenes[8] ($R_1R_2C(OH)CH_2C{\equiv}CH$). The experimental data show that these reactions are homogeneous and unimolecular and follow a first-order rate law.

The values of the entropies of activation ($\Delta S^{\ddagger} < 0$) are typical of those reactions that are thought to involve a cyclic transition state.[9]

The available experimental results are listed in Table 1 for the secondary and tertiary alcohols. The experimental thermolysis for the primary alcohol has not been studied. The tertiary alcohol decomposes more readily than the secondary. The experimental relative rates secondary/tertiary are 1.0:4.4, at 320 °C.[2] This behavior is similar to that observed in β-hydroxyketones, relative rates 1.0:4.2, at 230 °C,[6] and although less pronounced, in β-hydroxyolefins, 1.0:1.9, at 377 °C,[7] and in β-hydroxyacetylenes, 1.0:1.3, at 350 °C.[8]

TABLE 1: Comparative Rates and Activation Parameters at 320 °C

substrate	10^4 k, s^{-1}	E_a, kJ mol^{-1}	log A	ref
ethyl 3-hydroxybutanoate, **II**	2.32	166.1	10.98	2
ethyl 3-hydroxy-3-methyl-butanoate, **III**	50.12	155.9	11.43	1
	10.20	161.0	11.20	2
	10.47	174.5 ± 5.2	12.39 ± 0.46	4

Previous studies have been devoted to study the thermolysis of β-hydroxyketones,[10] β-hydroxyolefins,[11] and β-hydroxyacetylenes,[12] but to our knowledge, there is not any previous theoretical study on the thermolysis reactions of ethyl β-hydroxycarboxylates.

In this paper, we present a theoretical study of the thermal decomposition in the gas phase of three ethyl β-hydroxycarboxylates: ethyl-3-hydroxypropionate (primary alcohol, **I**), ethyl-3-hydroxybutanoate (secondary alcohol, **II**), and ethyl-3-hydroxy-3-methylbutanoate (tertiary alcohol, **III**). We have studied the principal and side reactions and have compared the theoretical results with the available experimental data. This study was carried out using ab initio analytical gradients at the MP2 level of theory[13] with the 6-31G(d)[14] and 6-311++G(2d,p)[15] basis sets.

* To whom correspondence should be addressed. Fax: 34−91−5642431. E-mail: rnotario@iqfr.csic.es.
† Instituto de Química Física "Rocasolano".
‡ Universidad Nacional de Colombia.
§ Universidad de Chile.

10.1021/jp020071f CCC: $22.00
Published on Web 04/06/2002

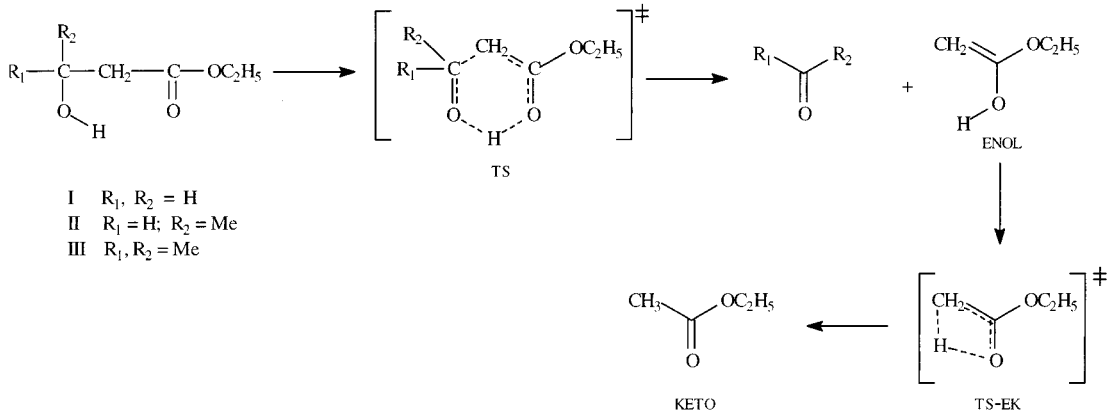

Figure 1. Mechanism of the decomposition of ethyl β-hydroxycarboxylates suggested form experiments.

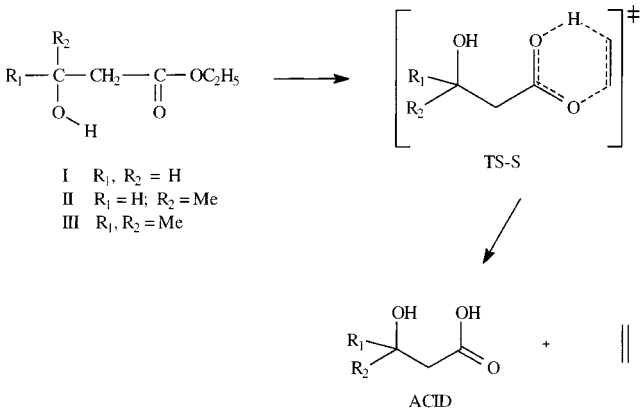

Figure 2. Side reactions studied in this work.

Computational Details

All calculations have been performed with the Gaussian 98 computational package.[16] The geometric parameters for all the reactants, the transition states (TS), and the products of the two pathways of the three studied reactions were fully optimized at the MP2/6-31G(d) level,[14] to obtain the energy profiles corresponding to the three studied reactions. Each stationary structure was characterized as a minimum or a saddle point of first order by frequency calculations. A scaling factor[17] of 0.9670 for the zero-point vibrational energies has been used.

Intrinsic reaction coordinate (IRC) calculations[18] have been performed in all cases to verify that the localized transition state structures connect with the corresponding minimum stationary points associated with reactants and products.

In the case of the reactants **I**, **II**, and **III** and the transition states **TS**−**I**, **TS**−**II**, and **TS**−**III**, corresponding to the first step of the principal reactions, single-point energy calculations at the MP2/6-311++G(2d,p) level[15] were also carried out.

The bonding characteristics of the different reactants, transition states, and products have been investigated using a population partition technique: the natural bond orbital (NBO) analysis of Reed and Weinhold.[19,20] The NBO formalism provides values for the atomic natural total charges and also provides the Wiberg bond indices[21] used to follow the progress of the reactions. The NBO analysis has been performed using the NBO program,[22] implemented in the Gaussian 98 package,[16] and has been carried out on the MP2 charge densities in order to explicitly include electron correlation effects.

We have selected the classical transition state theory (TST)[9,23] to calculate the kinetic parameters. The rate constant, $k(T)$, for each elementary step of the kinetic scheme (see Figures 1 and 2) was computed using this theory assuming that the transmission coefficient is equal to unity, as expressed by the following relation:

$$k(T) = (k_B T/h) \exp[-\Delta G^{\ddagger}(T)/RT] \quad (1)$$

where k_B, h, and R are the Boltzman constant, the Planck constant, and the universal gas constant, respectively. $\Delta G^{\ddagger}(T)$ is the standard-state free energy of activation, at the absolute temperature T.

The activation energies, E_a, and the Arrhenius A factors have been calculated using eqs 2 and 3, respectively, derived from the TST theory:

$$E_a = \Delta H^{\ddagger}(T) + RT \quad (2)$$

$$A = e k_B T/h \exp[\Delta S^{\ddagger}(T)/R] \quad (3)$$

Results and Discussion

Theoretical calculations at the MP2/6-31G(d) level of theory have been carried out in order to explore the nature of the reaction mechanism for the unimolecular decomposition of ethyl β-hydroxycarboxylates in the gas phase. We have considered two competitive reaction pathways, represented in Figures 1 and 2.

The first pathway (see Figure 1) describes a two-step mechanism. The first step is a concerted process in which an aldehyde, or a ketone, and an enol intermediate are formed via a six-membered cyclic transition state, **TS**, where the hydrogen atom of the hydroxylic group is migrating to the oxygen atom of the carbonyl group. The second step is the tautomerization of the enol intermediate to ethyl acetate, through a 1,3-hydrogen shifting process via a four-membered cyclic transition state. The first step is slower than the second one, and so it is the rate-limiting step of the global process.

The second pathway (see Figure 2) is a one-step concerted process in which ethylene and a carboxylic acid are formed via a six-membered cyclic transition state, **TS**−**S**, where one of the hydrogen atoms of the CH_3 of the ethoxy group is migrating to the oxygen atom of the carbonyl group. This process is similar to the well-known decomposition of ethyl acetate itself,[24,25] in which ethylene and acetic acid are formed.

Electronic energies, zero-point vibrational energies, thermal correction to enthalpies, and entropies, evaluated at the MP2/6-31G(d) and in some cases MP2/6-311++G(2d,p)//MP2/6-31G(d) levels of theory, for all the reactants, transition states,

TABLE 2: Electronic Energies, Evaluated at the MP2/6-31G(d) and MP2/6-311++G(2d,p) Levels, Zero-Point Vibrational Energies, ZPE, and Thermal Corrections to Enthalpies, TCH, in Hartrees, and Entropies, *S*, in cal mol^{-1} K^{-1}, for All of the Reactants, Transition States, and Products Involved in the Studied Reactions

species	MP2/6-31G(d)	MP2/6-311++G(2d,p)// MP2/6-31G(d)	ZPE[a]	TCH[a]	*S*[a]
I	−420.938258	−421.305749	0.156510	0.187826	130.960
TS−I	−420.854027	−421.227320	0.150981	0.181862	128.516
ENOL	−306.683755		0.120314	0.145265	112.458
H_2CO	−114.167748		0.027283	0.035654	65.222
TS-EK	−306.614961		0.115855	0.139322	108.323
KETO	−306.744107		0.121596	0.145962	112.663
TS−SI	−420.836591		0.148513	0.180298	133.939
ACID-I	−342.602524		0.097949	0.120085	106.394
C_2H_4	−78.285028		0.052039	0.062259	67.593
II	−460.111032	−460.515651	0.185058	0.221263	142.587
TS−II	−460.031166	−460.441420	0.179533	0.215175	139.419
MeCHO	−153.346919		0.056951	0.069636	80.342
TS−SII	−460.009866		0.177254	0.213747	144.405
ACID-II	−381.785374		0.126848	0.153677	117.865
III	−499.283997	−499.725690	0.213579	0.254663	152.994
TS−III	−499.206225	−499.653719	0.207944	0.248537	150.192
Me_2CO	−192.523905		0.085926	0.103605	95.096
TS−SIII	−499.183471		0.205788	0.247115	155.692
ACID-III	−420.948013		0.155064	0.186923	128.221

[a] Evaluated at 593.15 K and 0.04 atm, at the MP2/6-31G(d) level.

and products involved in the two pathways of the three studied reactions are collected in Table 2.

Free Energy Profiles. Free energy profiles for the decomposition processes of the three studied ethyl β-hydroxycarboxylates are presented in Figure 3, obtained at the MP2/6-31G(d) level.

At first sight, it appears clearly that the formation of enol and a carbonyl compound is kinetically more favorable than the formation of ethylene and a carboxylic acid (**TS−S** transition states are higher than the **TS** ones), according to the experimental facts.[4] Once the enol is formed, via a low barrier, then the carbonyl compound and enol separate in the gas phase and the rearrangement of enol via the 1,3-hydrogen shift is the only possible pathway forming ethyl acetate. The rate of this second step then is not a factor in determining which of the two pathways is preferred.

The calculated activation free energies are 212.0, 202.1, and 195.5 kJ mol^{-1} for the reactions via the transition states **TS−I**, **TS−II**, and **TS−III**, respectively, whereas values of 240.5, 242.0, and 238.1 kJ mol^{-1} are calculated in the case of the formation of ethylene via the transition states **TS−SI**, **TS−SII**, and **TS−SIII**, respectively.

The overall process is exergonic, with reaction free energies of −62.8, −86.9, and −106.8 kJ mol^{-1} for reactions I, II, and III, respectively.

Principal Reactions. The theoretical mechanism for the first step of the principal reaction is presented in Figure 4. The reaction occurs via a six-membered cyclic transition state.

There is one and only one imaginary vibrational frequency in the transition states for the first step of the studied thermal decomposition reactions (410.9i, 501.4i, and 579.5i cm^{-1} for **TS−I**, **TS−II**, and **TS−III**, respectively, evaluated at the MP2/6-31G(d) level of theory, with the lowest real frequency being 62.2, 64.1, and 60.6 cm^{-1} for **TS−I**, **TS−II**, and **TS−III**, respectively). The optimized structures for these transition states show a "quasiplanar" geometry in all of the cases.

Table 3 shows the main distances for each optimized structure. During the thermolysis process, when the reactant is being transformed into its transition state, the O_1-C_2, C_3-C_4, and O_5-H_6 distances are increasing, whereas the C_2-C_3, C_4-O_5, and H_6-O_1 distances are decreasing.

TABLE 3: Main Distances, in Angstroms, in the Reactants and Transition States of the First Step of the Principal Reactions, Calculated at the MP2/6-31G(d) Level

	distance, Å					
	O_1-C_2	C_2-C_3	C_3-C_4	C_4-O_5	O_5-H_6	H_6-O_1
I	1.227	1.508	1.525	1.420	0.975	2.090
TS−I	1.322	1.379	2.141	1.265	1.523	1.043
II	1.227	1.508	1.529	1.424	0.977	2.040
TS−II	1.317	1.381	2.136	1.273	1.470	1.058
III	1.228	1.508	1.538	1.429	0.978	2.000
TS−III	1.314	1.383	2.149	1.279	1.436	1.072

To avoid the subjective aspects associated to the geometrical analysis of the transition states, the progress of the reactions has been followed by means of the Wiberg bond indices,[21] B_i. The bond index between two atoms is a measure of the bond order and, hence, of the bond strength between these two atoms. Thus, if the evolution of the bond indices corresponding to the bonds being made or broken in a chemical reaction is analyzed along the reaction path, a very precise image of the timing and extent of the bond-breaking and the bond-making processes at every point can be achieved.[26]

The Wiberg bond indices corresponding to the bonds being made or broken in the studied reactions for the reactants, transition states, and products are collected in Table 4.

To perform the bond index analysis, it is convenient to define[26] a relative variation of the bond index at the transition state, δB_i, for every bond, i, involved in a chemical reaction as

$$\delta B_i = (B_i^{TS} - B_i^{R})/(B_i^{P} - B_i^{R}) \quad (4)$$

where the superscripts R, TS, and P refer to reactants, transition states, and products, respectively.

The percentage of evolution of the bond order through the chemical step has been calculated by means of[27]

$$\%EV = 100\delta B_i \quad (5)$$

and the values are collected in Table 4.

For **TS−I**, it can be seen that the H_6 displacement from O_5 to O_1 is very advanced. The O_5-H_6 bond is almost broken (80.4%) while the H_6-O_1 bond is almost formed (70.4%).

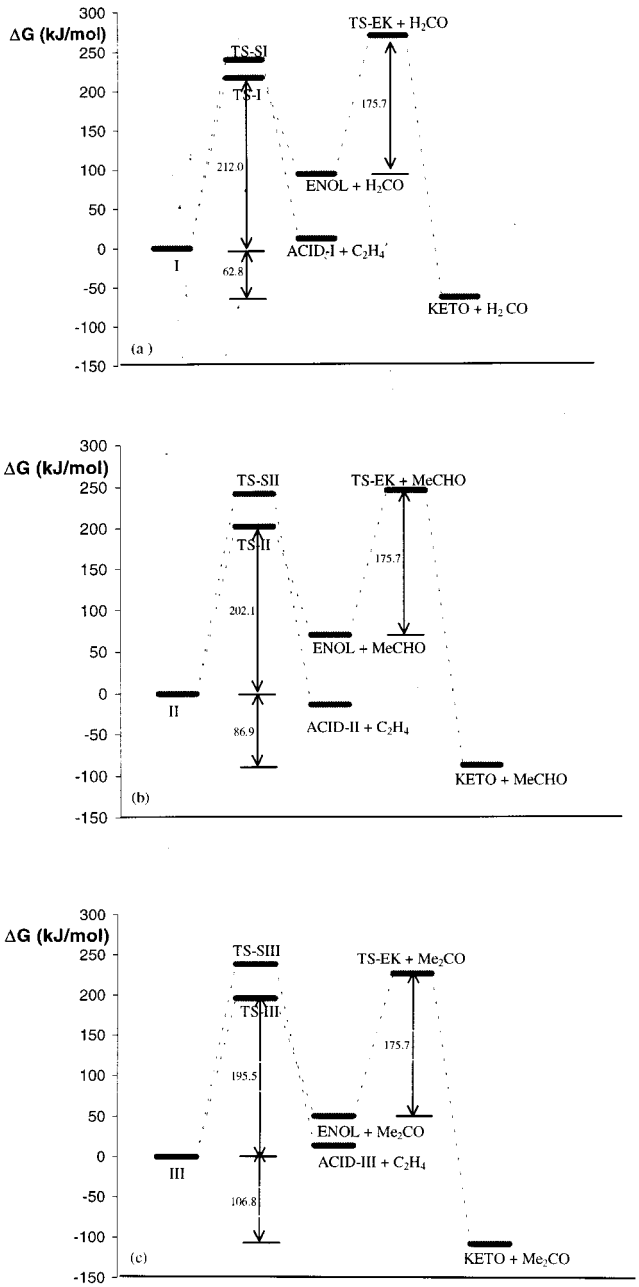

Figure 3. Free energy profiles at 593.15 K, evaluated at the MP2/6-31G(d) level, for the (a) I, (b) II, and (c) III decomposition process. (a) Relative free energy values (to reactant **I**, in kJ mol^{-1}) of the stationary points found are as follows: **TS**−**I**, 212.0; **TS**−**SI**, 240.5; **ACID-I** + C_2H_4, 12.5; **ENOL** + H_2CO, 94.5; **TS-EK** + H_2CO, 270.1; **KETO** + H_2CO, −62.8 (b) Relative free energy values (to reactant **II**, in kJ mol^{-1}) of the stationary points found are as follows: **TS**−**II**, 202.1; **TS**−**SII**, 242.0; **ACID-II** + C_2H_4, −13.2; **ENOL** + MeCHO, 70.3; **TS-EK** + MeCHO, 246.0; **KETO** + MeCHO, −86.9 (c) Relative free energy values (to reactant **III**, in kJ mol^{-1}) of the stationary points found are as follows: **TS**−**III**, 195.5; **TS**−**SIII**, 238.1; **ACID-III** + C_2H_4, 13.7; **ENOL** + Me_2CO, 50.4; **TS-EK** + Me_2CO, 226.1; **KETO** + Me_2CO, −106.8.

Furthermore, the O_1-C_2 double bond breaking is also advanced (79.4%). The breaking of the C_3-C_4 bond is 65.7% advanced, while the C_2-C_3 and C_4-O_5 double bonds formation is less advanced, only 57.0 and 52.1%, respectively.

The enlargement of the O_1-C_2 bond with the initial migration of the H_6 atom from O_5 to O_1 can be seen as the driving force for the studied reaction.

For **TS**−**II** and **TS**−**III**, the results are very similar to those obtained for **TS**−**I**, with the migration of the H_6 atom being slightly less advanced (see Table 4) going from the primary to the tertiary alcohol.

TABLE 4: Wiberg Bond Indices, B_i, of Reactants, Transition States, and Products of the First Step of the Principal Reactions, and Percentage of Evolution, %EV, through the Chemical Process of the Bond Indices at the Transition States

		O_1-C_2	C_2-C_3	C_3-C_4	C_4-O_5	O_5-H_6	H_6-O_1
reaction I	B_i^R	1.662	0.996	1.003	0.930	0.715	0.015
	B_i^{TS}	1.102	1.475	0.344	1.420	0.140	0.514
	B_i^P	0.957	1.837	0.000	1.871	0.000	0.724
	%EV	79.4	57.0	65.7	52.1	80.4	70.4
reaction II	B_i^R	1.659	0.998	0.992	0.913	0.708	0.017
	B_i^{TS}	1.118	1.461	0.348	1.374	0.164	0.487
	B_i^P	0.957	1.837	0.000	1.822	0.000	0.724
	%EV	77.1	55.2	64.9	50.7	76.8	66.5
reaction III	B_i^R	1.652	0.997	0.978	0.905	0.704	0.020
	B_i^{TS}	1.130	1.450	0.340	1.348	0.180	0.467
	B_i^P	0.957	1.837	0.000	1.785	0.000	0.724
	%EV	75.1	53.9	65.2	50.3	74.4	63.5

TABLE 5: Degree of Advancement of the Transition States, δB_{av}, and Absolute Synchronicities, Sy, in the First Step of the Principal Reactions

reaction	δB_{av}	Sy
I	0.675	0.918
II	0.652	0.924
III	0.637	0.926

The average value, δB_{av}, calculated as[26]

$$\delta B_{av} = 1/n \sum \delta B_i \qquad (6)$$

with n being the number of bonds involved in the reaction, affords a measure of the degree of advancement of the transition state along the reaction path.

Calculated δB_{av} values for the studied reactions are shown in Table 5. As it can be seen in this Table, the δB_{av} values show that the transition states are advanced, nearer to the products than to the reactants.

One can also obtain information on the absolute asynchronicity, A, of a chemical reaction, using the expression proposed by Moyano et al.:[26]

$$A = 1/(2n - 2) \sum |\delta B_i - \delta B_{av}|/\delta B_{av} \qquad (7)$$

The opposite to the asynchronicity, the synchronicity, Sy, defined as

$$\mathrm{Sy} = 1 - A \qquad (8)$$

varies between zero, when one of the n bonds has completely broken at the TS while the other $(n - 1)$ bonds remain completely unchanged, and one where all of the n bonds have broken or formed at exactly the same extent in the TS.

The Sy values obtained in this way are, in principle, independent of the degree of advancement of the transition state.

The Sy values calculated for the studied reactions are shown in Table 5. As it can be seen in this table, the synchronicities are higher than 0.9 in all of the cases, indicating that the mechanisms correspond to concerted and highly synchronous processes.

A last aspect to be taken into account is the relative asynchronicity of the bond-breaking and the bond-forming processes that it would be a measure of "bond deficiency" along the reaction path. In the studied reactions, the bond-breaking

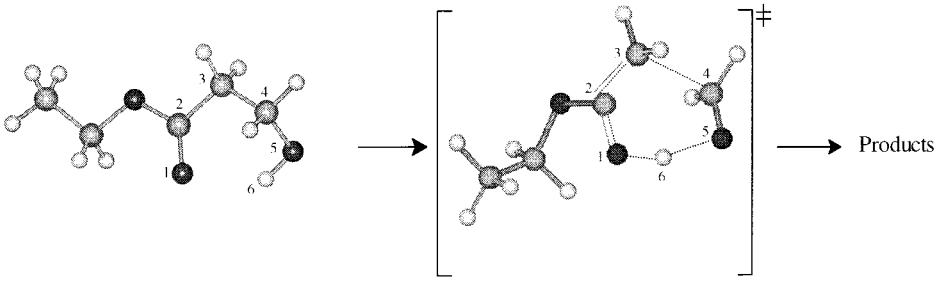

Figure 4. Theoretical mechanism of the first step of the principal reaction I, calculated at the MP2/6-31G(d) level.

TABLE 6: NBO Charges, Calculated at the MP2/6-31G(d) Level, at the Atoms Involved in the First Step of the Principal Reactions

	O_1	C_2	C_3	C_4	O_5	H_6
I	−0.736	1.006	−0.572	−0.032	−0.816	0.509
TS−I	−0.822	0.909	−0.727	0.273	−0.819	0.572
II	−0.737	1.012	−0.569	0.153	−0.828	0.513
TS−II	−0.826	0.911	−0.725	0.457	−0.835	0.574
III	−0.741	1.014	−0.566	0.329	−0.831	0.513
TS−III	−0.830	0.920	−0.738	0.642	−0.844	0.576

processes are more advanced than the bond-forming ones indicating a bond deficiency in the transition states.

The charge distribution in reactants and transition states has been analyzed by means of the natural bond orbital (NBO) analysis of Weinhold et al.[19,20] In Table 6, we have collected the natural atomic charges (the nuclear charges minus summed natural populations of the natural atomic orbitals on the atoms) at the atoms involved in the reaction.

Charges at **TS−I** show an important positive charge developed on H_6 (0.572 at TS and 0.509 at reactant) and on C_4 (0.273 at TS and −0.032 at reactant), whereas the electronic excess is supported by the two oxygens (−0.822 at TS and −0.736 at reactant, for O_1, and −0.819 at TS and −0.816 at reactant, for O_5) and by C_3 (−0.727 at TS and −0.572 at reactant). The negative character of O_1 allows it to attract the H_6 in the TS. The same hydrogen atom has a more positive character in the TS, and thus O_1 increases its negative character, and O_5 has a more negative character, as would expected by the postulated cyclic transition state. A very similar analysis can be made for **TS−II** and **TS−III**.

The kinetic parameters for the three reactions studied here have been calculated at the same temperature and pressure used in the experiments, 593.15 K and 0.04 atm. These data are compared with the experimental results (secondary and tertiary alcohols) in Table 7.

The results obtained at the MP2/6-311++G(2d,p)//MP2/6-31G(d) level of theory agree very well with the available experimental data, much better than the results obtained at the lower MP2/6-31G(d) level. This is a confirmation that the use of diffuse functions on hydrogen are necessary to get a good description of the migrating hydrogen in the transition states.

In Table 7, the negative values of the activation entropies indicate that these are typical of those reactions that are assumed to involve a cyclic TS, corroborating the experimentally postulated mechanism.

In a second step, the enol intermediate initially formed tautomerizes to the keto form, ethyl acetate. This step is faster than the first one ($k = 4.11 \times 10^{-3}$ s^{-1}), with an activation energy of 170.3 kJ mol^{-1} and an entropy of activation of −17.3 J mol^{-1} K^{-1}, evaluated at the MP2/6-31G(d) level. The transition state, **TS-EK**, that is common to the three studied reactions, presents one and only one imaginary vibrational frequency at 2152.1i cm^{-1} with a lowest real frequency of 107.6 cm^{-1}, evaluated at the MP2/6-31G(d) level of theory.

Side Reactions. We have carried out a theoretical study of an alternative mechanism of the thermal decomposition of the studied ethyl β-hydroxycarboxylates, giving as products ethylene and a carboxylic acid (see Figure 2). These reactions take place via a six-membered cyclic transition state.

There is one and only one imaginary vibrational frequency in these transition states, evaluated at the MP2/6-31G(d) level (1717.7i, 1717.4i, and 1710.1i cm^{-1}, for **TS−SI**, **TS−SII**, and **TS−SIII**, respectively, with the lowest real frequency being 23.9, 20.2, and 10.3 cm^{-1}, for **TS−SI**, **TS−SII**, and **TS−SIII**, respectively).

The activation energies calculated at the MP2/6-31G(d) level are 233.6, 234.7, and 233.6 kJ mol^{-1}, for the reactions I, II, and III, respectively, clearly higher than the E_a values calculated for the principal reactions (see Table 7). The rate constants calculated at the same level of theory for these side reactions are 1.24×10^{-7}, 7.20×10^{-8}, and 2.11×10^{-7} s^{-1}, for the reactions I, II, and III, respectively.

Kinetic Isotope Effects. We have also carried out a theoretical study on the kinetic deuterium isotope effects in the thermal decomposition of the studied ethyl β-hydroxycarboxylates, and have compared the results with the experimental ones previously measured by one of us.[28,29]

The kinetic isotope effects, k_H/k_D, obtained at the MP2/6-31G(d) and MP2/6-311++G(2d,p)//MP2/6-31G(d) levels of theory, are shown in Table 8.

The experimental primary isotope effect in **III** suggests that the previously proposed six-membered cyclic transition state, characterized by partial bonds between H (or D) and the two oxygens of the carbonyl and the hydroxyl groups is correct. It is known that the magnitude of the primary isotope effect in a hydrogen-transfer reaction varies with the symmetry of the transition state and it is maximum when the hydrogen is symmetrically bonded to the atoms between which is being transferred. The small value of this effect (see Table 8) is a consequence of the fact that the transfer of hydrogen, partially bonded to the oxygen of the carbonyl and hydroxyl groups in the TS, is not linear, and the TS is late (see the previous discussion on the character of the transition states, using the Wiberg bond indices). The O−H is not stretched to its breaking point, but it does bend, so the hydrogen atom may become attached to another part of the molecule. It is the bending rather than the stretching which is connected into translation motion.[30,31] Because vibration frequencies for bending are much lower than those for stretching, the zero-point energy lost in the transition state will be small, and therefore, the primary kinetic deuterium effect should be small.

As it can be seen in Table 8, the primary effect increases in the order primary alcohol < secondary alcohol < tertiary alcohol.

TABLE 7: Theoretical and Experimental Kinetics and Activation Parameters for the Pyrolysis of Ethyl β-Hydroxycarboxylates in the Gas Phase, at 593.15 K

	10^4 k, s^{-1}		E_a, kJ mol^{-1}		log A		$\Delta H^{\ddagger}$, kJ mol^{-1}		$\Delta G^{\ddagger}$, kJ mol^{-1}		$\Delta S^{\ddagger}$, J mol^{-1} K^{-1}	
alcohol	calc[a]	exp[b]	calc[a]	exp[b]	calc[a]	exp[b]	calc[a]	exp[b]	calc[a]	exp[b]	calc[a]	exp[b]
primary	0.39		197.6		13.0		192.7		198.7		−10.2	
I	(0.026)		(210.9)				(206.0)		(212.0)			
secondary	2.50	2.32	186.5	166.1	12.8	10.98	181.6	161.2	189.5	189.9	−13.3	−48.7
II	(0.20)		(199.1)				(194.2)		(202.0)			
tertiary	9.55	10.47	180.8	174.5 ± 5.2	12.9	12.39 ± 0.46	175.9	169.6	182.9	182.4	−11.7	−21.8
III	(0.74)		(193.5)				(188.6)		(195.5)			

[a] Values calculated at the MP2/6-311++G(2d,p)//MP2/6-31G(d) and, in parentheses, MP2/6-31G(d) levels. [b] The values for the secondary compound are taken from ref 2, and for the tertiary compound, the values are taken from ref 4.

TABLE 8: Kinetic Deuterium Isotope Effects, k_H/k_D, in the Pyrolysis of Ethyl β-Hydroxycarboxylates in the Gas Phase, at 479.15 K

effect	MP2/6-31G(d)	MP2/6-311++G(2d,p)// MP2/6-31G(d)	expt
	Reaction I		
primary	1.53	1.49	
α-secondary	1.28	1.28	
	Reaction II		
primary	1.69	1.70	
α-secondary	1.13	1.13	
β-secondary	1.02	1.03	
	Reaction III		
primary	1.74	1.78	1.97[a]
α-secondary	1.08	1.11	1.26[b]
β-secondary	1.11	1.11	1.52[a]

[a] Value taken from ref 28. [b] Value taken from ref 29.

The α-secondary deuterium isotope effects that occur when deuterium atoms are attached to a center that is undergoing a hybridization change are small but higher than unity (see Table 8). These results are a consequence that in the proposed mechanism the C_3 and C_4 atoms change their hybridization from sp^3 in the reactants to sp^2 in the transition states. According to the Streitweiser model,[32] the alpha isotope effect is predominantly due to the change of a tetrahedral C−H bending vibration to an "out of plane" deformation in the TS.

By observing the values of the β-secondary deuterium isotope effects (see Table 8), they represent exclusively β-secondary effects because H (or D) atoms attached to the carbon atoms are not lost in the rate-limiting step.

As it can be seen in Table 8, the α- and β-secondary effects are cumulative and depend of the number of H_α and H_β in the molecules. So, the α-secondary effect increases in the order reaction III < reaction II < reaction I, in the same order that the number of H_α increases (two in reactant **III**, three in **II**, and four in **I**), whereas the β-secondary effect is small but slightly higher in reaction III (six H_β in reactant **III**) than in reaction II (three H_β in **II**), and there is no β-secondary effect in reaction I (there is no H_β in reactant **I**).

Conclusions

A theoretical study on the thermal decomposition in the gas phase of three ethyl β-hydroxycarboxylates has been carried out. The free energy profiles, evaluated at the MP2/6-31G(d) level of theory, show clearly that the formation of ethyl acetate and a carbonyl compound is kinetically more favorable than the formation of ethylene and a carboxylic acid, according to experimental facts.

The principal reactions take place via a six-membered cyclic transition state. The progress of the reactions has been followed by means of the Wiberg bond indices. The enlargement of the O_1-C_2 bond with the initial migration of the H_6 atom from O_5 to O_1 can be seen as the driving force for the studied reactions. The transition states are late, nearer to the products than to the reactants. The calculated synchronicities show that the reactions are concerted and highly synchronous. The bond-breaking processes are more advanced than the bond-forming ones, indicating a bond deficiency in the transition states.

The kinetic parameters for the studied reactions, evaluated at the MP2/6-311++G(2d,p)//MP2/6-31G(d) level, agree very well with the available experimental data.

A theoretical study on the kinetic deuterium isotope effects has also been carried out comparing the results with the available experimental data. All of the effects are in accord with the postulated mechanism of the reactions.

Acknowledgment. This work was supported by research funds provided by CINDEC (Comité de Investigación y Desarrollo Científico, Universidad Nacional de Colombia, Sede Medellín), COLCIENCIAS (Instituto Colombiano para el Desarrollo de la Ciencia y la Tecnología; Project No. 1118-05-11481), and the Spanish Dirección General de Investigación, Ministerio de Ciencia y tecnología (Project No. BQU20001499). The authors also thank COLCIENCIAS and C.S.I.C. for the joint project No. 2001CO0004. E.C. thanks Fondecyt Grant No. 2990030 and to Universidad de Chile-Mecesup Grant UCH0008. R. N. thanks CESGA and CESCA for computing facilities.

References and Notes

(1) Yates, B. L.; Quijano, J. *J. Org. Chem.* **1970**, *35*, 1239.
(2) Yates, B. L.; Ramírez, A.; Velásquez, O. *J. Org. Chem.* **1971**, *36*, 3579.
(3) August, R.; McEwen, I.; Taylor, R. *J. Chem. Soc., Perkin Trans. 2* **1987**, 1683.
(4) Domínguez, R. M.; Chuchani, G.; Quijano, J.; Orozco, L. J.; Restrepo, I. *React. Kinet. Catal. Lett.* **1996**, *57*, 191.
(5) Yates, B. L.; Quijano, J. *J. Org. Chem.* **1969**, *34*, 2506.
(6) Rotinov, A.; Chuchani, G.; Machado, R. A.; Rivas, C.; Quijano, J.; Yepes, M. S.; Restrepo, I. *Int. J. Chem. Kinet.* **1992**, *24*, 909.
(7) Smith, G. G.; Yates, B. L. *J. Chem. Soc.* **1965**, 7242.
(8) Viola, A.; MacMillan, J. H.; Proverb, R. J.; Yates, B. L. *J. Am. Chem. Soc.* **1971**, *93*, 6967.
(9) Benson, S. W. *The Foundations of Chemical Kinetics*; McGraw-Hill: New York, 1969.
(10) Feng, W.; Wang, Y.; Zhang, S. *Int. J. Quantum Chem.* **1997**, *62*, 297.
(11) Quijano, J.; David, J.; Sánchez, C.; Rincón, E.; Guerra, D.; León, L. A.; Notario, R.; Abboud, J. L. *J. Mol. Struct. (THEOCHEM)* **2002**, in press.
(12) Quijano, J.; Sánchez, C.; David, J.; Rincón, E.; León, L. A.; Notario, R.; Abboud, J.-L. M. *J. Mol. Struct. (THEOCHEM)* **2001**, *572*, 135.
(13) Møller, C.; Plesset, M. *Phys. Rev.* **1934**, *46*, 618.
(14) Ditchfield, R.; Hehre, W. J.; Pople, J. A. *J. Chem. Phys.* **1971**, *54*, 724.
(15) Clark, T.; Chandrasekhar, J.; Spitznagel, G. W.; Schleyer, P. v. R. *J. Comput. Chem.* **1983**, *4*, 294.
(16) Frisch, M. J.; Trucks, G. W.; Schlegel, H. B.; Scuseria, G. E.; Robb, M. A.; Cheeseman, J. R.; Zakrzewski, V. G.; Montgomery, J. A., Jr.; Stratmann, R. E.; Burant, J. C.; Dapprich, S.; Millam, J. M.; Daniels, A.

D.; Kudin, K. N.; Strain, M. C.; Farkas, O.; Tomasi, J.; Barone, V.; Cossi, M.; Cammi, R.; Mennucci, B.; Pomelli, C.; Adamo, C.; Clifford, S.; Ochterski, J.; Petersson, G. A.; Ayala, P. Y.; Cui, Q.; Morokuma, K.; Malick, D. K.; Rabuck, A. D.; Raghavachari, K.; Foresman, J. B.; Cioslowski, J.; Ortiz, J. V.; Stefanov, B. B.; Liu, G.; Liashenko, A.; Piskorz, P.; Komaromi, I.; Gomperts, R.; Martin, R. L.; Fox, D. J.; Keith, T.; Al-Laham, M. A.; Peng, C. Y.; Nanayakkara, A.; Gonzalez, C.; Challacombe, M.; Gill, P. M. W.; Johnson, B. G.; Chen, W.; Wong, M. W.; Andres, J. L.; Head-Gordon, M.; Replogle, E. S.; Pople, J. A. *Gaussian 98*, revision A.9; Gaussian, Inc.: Pittsburgh, PA, 1998.

(17) Scott, A. P.; Radom, L. *J. Phys. Chem.* **1996**, *100*, 16502.

(18) Fukui, K. *J. Phys. Chem.* **1970**, *74*, 4161.

(19) Reed, A. E.; Weinhold, F. *J. Chem. Phys.* **1983**, *78*, 4066.

(20) Reed, A. E.; Curtiss, L. A.; Weinhold, F. *Chem. Rev.* **1988**, *88*, 899.

(21) Wiberg, K. B. *Tetrahedron* **1968**, *24*, 1083.

(22) Glendening, E. D.; Reed, A. E.; Carpenter, J. E.; Weinhold, F. *NBO*, version 3.1.

(23) Glasstone, K. J.; Laidler, K. J.; Eyring, H. *The Theory of Rate Processes*; McGraw-Hill: New York, 1941; Chapter 4.

(24) Beadle, P. C.; Golden, D. M.; Benson, S. W. *Int. J. Chem. Kinet.* **1972**, *4*, 265.

(25) Lee, I.; Cha, O. J.; Lee, B.-S. *J. Phys. Chem*. **1990**, *94*, 3926.

(26) Moyano, A.; Pericàs, M. A.; Valentí, E. *J. Org. Chem.* **1989**, *54*, 573.

(27) Domingo, L. R.; Picher, M. T.; Safont, V. S.; Andrés, J.; Chuchani, G. *J. Phys Chem. A* **1999**, *103*, 3935.

(28) Quijano, J.; Rodríguez, M. M.; Yepes, M. S.; Gallego, L. H. *Tetrahedron. Lett.* **1987**, *28*, 3555.

(29) Quijano, J.; Restrepo, I.; Gallego, L. H.; Yepes, M. S. *Tetrahedron. Lett.* **1994**, *35*, 4735.

(30) Westheimer, F. H. *Chem. Rev.* **1961**, *61*, 265.

(31) More O'Ferrall, R. A. *J. Chem. Soc. B* **1970**, 785.

(32) Streitweiser, A., Jr.; Jagow, R. H.; Fahey, R. C.; Suzuki, S. *J. Am. Chem. Soc.* **1958**, *80*, 2326.